



Published in final edited form as:

J Thorac Cardiovasc Surg. 2020 May ; 159(5): 1825–1835.e2. doi:10.1016/j.jtcvs.2019.06.017.

Delayed delivery of endothelial progenitor cell derived extracellular vesicles via shear-thinning gel improves post-infarct hemodynamics

Jennifer J. Chung, Jason Han, Leo L. Wang, Maria F. Arisi, Samir Zaman, Jonathan Gordon, Elizabeth Li, Samuel T. Kim, Zoe Tran, Carol W. Chen, Ann C. Gaffey, Jason A. Burdick, Pavan Atluri

Division of Cardiovascular Surgery, Departments of Surgery and Bioengineering, University of Pennsylvania, Philadelphia, PA.

Abstract

Background—EVs are promising therapeutics for cardiovascular disease, but poorly-timed delivery may hinder efficacy. We characterized the time-dependent response to EPC-EVs within an injectable shear-thinning hydrogel (STG+EV) post-MI to identify when an optimal response is achieved.

Methods—The angiogenic effects of prolonged hypoxia on cell response to EPC-EV therapy and EV uptake affinity were tested *in vitro*. A rat model of acute MI via LAD ligation was created and STG+EV was delivered via intramyocardial injections into the infarct borderzone at timepoints corresponding to phases of post-MI inflammation – 0h (immediate), 3h (acute inflammation), 4d (proliferative), and 2wk (fibrosis). Hemodynamics 4 weeks post-treatment were compared across treatments and controls (PBS, STG). Scar thickness and ventricular diameter were assessed histologically. Primary hemodynamic endpoint was end systolic elastance. The secondary endpoint was scar thickness.

Results—EPC-EVs incubated with chronically vs. acutely hypoxic HUVECS resulted in a 2.56 ± 0.53 vs 1.65 ± 0.15 -fold increase ($p=0.05$) in number of vascular meshes and higher uptake of EVs over 14 hours. Ees improved with STG+EV therapy at 4d (0.54 ± 0.08) vs PBS or STG (0.26 ± 0.03 , $p=0.02$; 0.23 ± 0.02 , $p=0.008$). Preservation of ventricular diameter ($6.20 \text{mm} \pm 0.73$ vs. $8.58 \text{mm} \pm 0.38$, $p=0.04$; $9.13 \text{mm} \pm 0.25$, $p=0.01$) and scar thickness ($0.885 \text{mm} \pm 0.046$ vs. $0.615 \text{mm} \pm 0.029$, $p<0.0001$ and $0.577 \text{mm} \pm 0.052$, $p<0.0001$) was significantly greater at 4d, compared to PBS and STG controls.

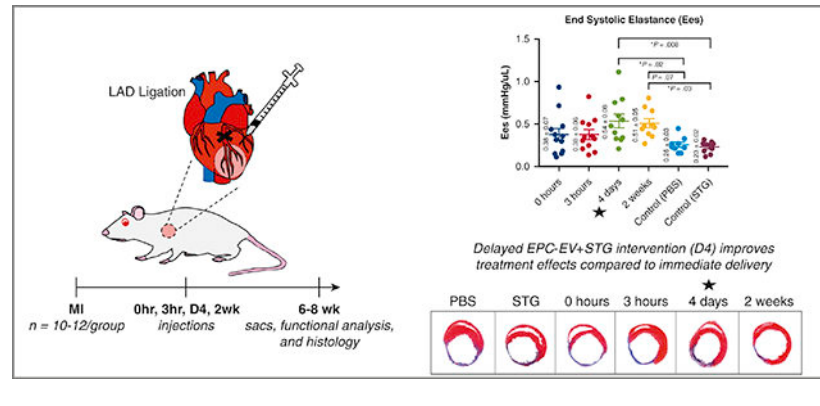
Correspondence: Pavan Atluri, M.D., Associate Professor of Surgery, Director, Minimally Invasive and Robotic Cardiac Surgery, Director, Heart Transplantation and Mechanical Circulatory Support Program, Division of Cardiovascular Surgery, Department of Surgery, University of Pennsylvania, 6 Silverstein Pavilion, 3400 Spruce Street, Philadelphia, PA 19104, pavan.atluri@uphs.upenn.edu, Phone: 215-662-2956.

Disclosure: None of the authors have any conflicts of interest

Publisher's Disclaimer: This is a PDF file of an unedited manuscript that has been accepted for publication. As a service to our customers we are providing this early version of the manuscript. The manuscript will undergo copyediting, typesetting, and review of the resulting proof before it is published in its final citable form. Please note that during the production process errors may be discovered which could affect the content, and all legal disclaimers that apply to the journal pertain.

Conclusions—Delivery of STG+EV 4 days post-MI improves LV contractility and preserves global ventricular geometry, compared to controls and immediate therapy post-MI. These findings suggest other cell-derived therapies can be optimized by strategic timing of therapeutic intervention.

Graphical Abstract



BACKGROUND

Extracellular vesicles (EVs) are lipid-membrane bound particles that are actively released from cells and carry cargo of various RNA species, proteins and bioactive lipids.¹ EVs have garnered significant interest as a novel therapeutic for vascular regeneration after ischemic injury, including myocardial infarction (MI).² Numerous publications have found that EVs derived from progenitor or stem cells can recapitulate the beneficial effects of these cell therapies.^{1,3,4} However, there is little data exploring the effect of the timing of intervention on outcomes after EV therapy.

Ischemia alters cell metabolism and function and can lead to irreversible injury and cell death. Surviving cells are exposed to a wide range of evolving inflammatory, neurohormonal and paracrine effects that drive cardiac fibrosis and remodeling.⁵ Given that the substrate upon which EVs act is the recipient cell, we hypothesized that the cell microenvironment would affect EV uptake and therapeutic efficacy after MI.

We have previously described how EVs derived from endothelial progenitor cells (EPCs) produce the same therapeutic benefits as EPCs themselves, namely improved hemodynamics; increased peri-infarct vascular density; and mitigation of deleterious post-MI remodeling.⁶ In our previous work, EPC-EVs were delivered within a shear-thinning gel (STG+EV), which is formed from biocompatible components binding via guest-host interactions.⁶⁻⁸ These bonds can be broken with shear stress and allow injection through a syringe, resulting in more precise targeting of EVs to the ischemic borderzone post-MI, as well as sustained delivery over at least 21 days. Using this novel construct of STG+EV, we designed the current study to parallel the phases of inflammation and healing after an ischemic insult – acute inflammation, proliferation, and fibrosis⁹ – to determine how changes in the timing of delivery of EPC-EVs affect functional results of this therapy.

METHODS

Animal Use

All experiments conform to the National Institute of Health Guide for Care and Use of Laboratory Animals and were approved by the Institutional Animal Care and Use Committee of the University of Pennsylvania. *Rattus norvegicus* fWistar) rats were obtained from Charles River Laboratories, Inc (Boston, MA).

Isolation of Endothelial Progenitor Cells

Adult Wistar rats (350–375g) received an intraperitoneal pentobarbital injection at 100 mg/kg. After cessation of pedal reflex, euthanasia was performed by transection of the carotid artery, and introduction of pneumothorax. Following exsanguination, the long bones were collected, and bone marrow was harvested.

Bone marrow mononuclear cells were isolated by density-gradient centrifugation on Histopaque-1083 (Sigma-Aldrich, 10831) and plated on vitronectin-coated 10-cm culture dishes. EPCs were cultured as the adherent fraction in 5% FBS EGM-2 (Lonza, Basel, Switzerland) without heparin or hydrocortisone. After 4 days, cells were washed twice to remove non-adherent cells.

Isolation of Extracellular Vesicles from EPCs and Storage

Four days post-isolation, EPCs were changed to serum-free EGM-2 without heparin or hydrocortisone. After 48 hours, the conditioned media (CM) was collected, centrifuged at 2000×G for 30 minutes, then clarified through a Stericup 0.22µm PVDF filtration unit (Millepore Sigma). Clarified conditioned media (CCM) was then incubated in a 1:2 ratio with 36% PEG, 1.5M NaCl overnight at 4°C, pelleted by centrifugation at 10,000×G 4°C for 2 hours, and re-suspended in sterile-filtered dPBS. EVs were stored at –80°C until use. EVs were re-suspended at a concentration of 9.33×10^{10} particles/ml for *in vivo* use, and at 1.87×10^{11} particles/ml for *in vitro* use (Figure 1). Samples that were too dilute were re-pelleted with ExoQuick-TC (System Biosciences, Palo Alto, CA) per manufacturer's instructions.

Shear-thinning Gel Synthesis

STG was formed by modifying hyaluronic acid (HA) with adamantine (Ad) and β-cyclodextrin (CD). The sodium salt of HA was dissolved in deionized water at 2% w/w, exchanged against Dowex-100 resin, neutralized by tetrabutylammonium hydroxide (TBA), frozen, and lyophilized to form HA-TBA. Hydrogels of 4% w/w were prepared from lyophilized polymers of Ad-HA and CD-HA dissolved in PBS and mixed. All reagents were manufactured by Sigma-Aldrich.

Tubule Formation Assay

To study the effects of prolonged ischemia on cell response to EPC-EV therapy *in vitro*, a subset of HUVECs were exposed to hypoxia (5% O₂) for 7 days. On day 7, a Matrigel tubule formation assay was performed under hypoxic conditions and response to EPC-EV therapy was compared between HUVECs that had been chronically hypoxic vs naïve cells.¹⁰

10 μ L of Matrigel (Corning, Cat #354234) was pipetted into the inner chamber of u-Angiogenesis slides (Ibidi, Cat#81506). After a 30-minute polymerization period at 37°C, experimental conditions and 1.2×10^4 HUVECs were added to each well. Groups included chronically hypoxic or naive cells with 4.68×10^8 EVs (2.5 μ l of 1.87×10^{11} particles/ml stock in 50 μ L EBM2), or vehicle control (2.5 μ l dPBS in EBM2). Serum free-EGM was used as a positive control. After 14 hours of incubation in 5% O₂, vascular mesh formation was visualized with the EVOS XL Imaging System (Invitrogen) under brightfield 4 \times magnification. Vascular meshes were quantified using ImageJ (NIH), and the response of cells to EVs was normalized to the vehicle control.^{11,12}

Labeled EV Uptake by HUVECs Under Acute vs. Chronic Hypoxic Conditions

EV action is predicated upon the uptake of secreted particles into a host cell.¹³ We therefore assessed the variation in HUVECs' ability to uptake EVs after a 4-day exposure to hypoxia (5% O₂) compared to that of naive HUVECs. EVs were labeled with 2 μ M DiI for 5 min at 37°C, and then 15 min at 4°C. Excess dye was removed with Exosome Spin Columns (MW=3000; Fisher Scientific Cat#4484449). 9.36×10^8 DiI-labeled EVs in serum free EGM2 were delivered to 1×10^4 HUVECs seeded in 8-well chamber slides. After 3 and 14 hours of incubation in 5% O₂, slides were washed in PBS three times, membranes were stained with WGA-AF647 for 15 min at room temperature, and nuclei were stained with DAPI. Images were taken on the Leica DM5000b upright fluorescent microscope at 40 \times magnification and processed on ImageJ. Mean fluorescent intensity was measured and normalized by the quantified area.

Histological Analysis

Hearts were explanted, embedded in OCT (Tissue Tek, Torrance, CA) and frozen on dry-ice. 10 μ m transverse sections were taken by cryosectioning at the mid-papillary muscle level. Sections were stained using Masson's Trichrome (Sigma-Aldrich). Scar thickness, a measure of LV remodeling, was determined by averaging the thickness at five equidistant points along the scar, using ImageJ. The LV diameter was measured from the midpoint of the septum to the midpoint of the opposite wall, along a perpendicular line, to determine post-infarction ventricular dilatation.

For H&E staining, hearts were explanted and fixed in 10% formalin at 4°C overnight, then embedded in paraffin. Hearts were sectioned and stained with H&E. Slides were analyzed with light microscopy at 4 \times and 10 \times magnification to assess cellular infiltration and inflammation.

Rat Model of Myocardial Infarction

An established rat model of MI induced by permanent occlusion of the left anterior descending artery (LAD) was used.¹⁴ Animals were randomized into 1 of 6 groups: PBS control ($n=10$); STG control ($n=10$); and STG+EV delivered at 0 hours ($n=11$), 3 hours ($n=12$), 4 days ($n=12$) or 2 weeks ($n=11$) after MI. Animals were induced with 5% isoflurane, intubated and mechanically ventilated, with 1–3% isoflurane to maintain a surgical anesthetic depth. Prior to incision, 0.05 mg/kg of buprenorphine was injected subcutaneously. Using a left 4th interspace thoracotomy, the LAD was identified and ligated

1 mm below the left atrial appendage with a resultant anterolateral MI encompassing 30% of the LV. At time of treatment, 100 μ L of STG containing 9.33×10^9 EVs was delivered via $5 \times 20 \mu$ L intramyocardial injections around the border zone of the infarcted area. The EPCs and EVs were allogenic and pooled from multiple donors. The 3h, 4d and 2w groups all underwent a second thoracotomy at the designated timepoint.

Measurement of Hemodynamics

Hemodynamic measures were obtained four weeks following treatment. After induction of anesthesia with 5% isoflurane, the rat was intubated and mechanically ventilated. Following confirmation of adequate surgical anesthesia maintained with continuous inhaled 2% isoflurane, a 2Fr pressure-volume (PV) catheter (Millar, Houston, TX) was inserted retrograde into the LV via the right common carotid artery, in a closed chest approach. Both steady-state hemodynamic parameters and end systolic elastance (Ees), were determined using the methods described by Pacher et al.¹⁵

Statistical Analysis

The primary endpoint is contractility, measured by Ees. Secondary endpoints are *in vitro* angiogenesis and scar thickness. Treatment groups were designated and coded by random identifiers. Investigators were blinded to treatment group during data acquisition and analysis. Values are expressed as mean \pm standard error of the mean (SEM). Comparison across experimental groups was performed by one-way analysis of variance (ANOVA). When a significant difference between groups was identified, pairwise comparison was performed using Tukey's HSD test. *P*-values <0.05 were considered statistically significant. Graphs show mean values with SEM.

RESULTS

Chronically hypoxic cells have a more robust angiogenic response to EPC-EVs

The *in vitro* hypoxic angiogenesis assay was designed to elucidate the impact of chronic hypoxia on cellular responses to EVs. A state of chronic hypoxia, such as that experienced by myocytes after an MI, was simulated by culturing cells in 5% O₂ for 7 days prior to a hypoxic Matrigel assay. The angiogenic stimulus of EPC-EVs to chronically vs. acutely hypoxic HUVECs revealed a 1.65 ± 0.15 vs 2.56 ± 0.53 -fold increase ($p=0.05$) in number of vascular meshes in the chronic hypoxia compared to the naïve group (Figure 2).

Chronic hypoxia increases EPC-EV uptake by HUVECs

We next examined the effect of hypoxia on cells' ability to take up EVs. DiI labelled EPC-EVs were incubated with HUVECs that had been maintained at either 5% O₂ for 4 days (preconditioned) or at 21% O₂ (naïve). After 14 hours, preconditioned HUVECs demonstrated significantly increased uptake of EVs compared to the naïve cells (0.11 ± 0.02 vs. 0.07 ± 0.01 , $p=0.01$) (Figure 3).

Inflammatory cell infiltrate most pronounced at 4 days post-MI

To better understand the evolution of the infarct and borderzone regions at each of the timepoints analyzed in this study, rat hearts were explanted at 0 hours, 3 hours, 4 days and 2 weeks after MI. H&E stained sections demonstrated a robust inflammatory cellular infiltrate present at 4 days post-MI with clear delineation between the borderzone and areas of irreversible cell injury and death, with areas of necrosis within the infarct. This necrosis progresses to fibrosis and thinning of the left ventricular wall and scar formation by 2 weeks (Figure 4).

STG+EV delivery at 4 days improves hemodynamics

PV catheter analysis demonstrated significant hemodynamic differences between the delayed treatment groups and controls. Ees, the slope of the end systolic pressure-volume relationship (ESPVR) measured during occlusion of the inferior vena cava, and is regarded as a volume-independent measure of contractility (Figure 5). Improvements in Ees were most pronounced after injection of STG+EV therapy at 4 days post-MI, with statistically significant improvement over PBS and STG controls (0.54 ± 0.08 vs. 0.26 ± 0.03 , $p=0.02$; 0.23 ± 0.02 , $p=0.008$) (Table 1). An alternate measure of contractility, maximum change in pressure over change in time (dp/dt_{max}) also showed improvement in the 4d group over PBS (5432 ± 309 mmHg/s vs. 3886 ± 397 , $p=0.033$). The 4d group also had statistically significantly higher ejection fraction (EF) compared to PBS and 0h groups ($59.6 \pm 1.4\%$ vs. $46.9 \pm 2.6\%$, $p=0.004$; 42.8 ± 2.8 , $p<0.0001$). Similarly, with regards to cardiac output, the 4d group showed statistically significant increases over PBS ($64,459 \pm 6308$ vs. $38,874 \pm 4929$, $p=0.016$), and 0h ($37,558 \pm 3549$, $p=0.007$). Furthermore, measures of LV relaxation were also markedly improved with therapy at 4d (-5443 ± 303), with statistically superior dp/dt_{min} compared with PBS (-3154 ± 347 , $p<0.0001$) and STG (-3942 ± 401 , $p=0.04$), as well as 0h (-3558 ± 465 , $p=0.003$) and 3h (-3762 ± 282 , $p=0.008$). The 2wk group also had superior dp/dt_{min} over PBS ($p=0.0001$), 0h ($p=0.003$) and 3h ($p=0.01$). To characterize the changing effects of treatment over time, a cohort of 4d and 2wk animals underwent hemodynamic assessment both at 4 and 6 weeks post-MI. Over time, the 4d group showed a mild decrease in EF at 4 vs 6 weeks post-treatment (59.6 ± 1.4 vs 53.7 ± 2.6 , $p=0.04$). In contrast, the 2wk group demonstrated a more significant decrement in EF from 4 weeks post-MI (2 weeks post-treatment) to 6 weeks post-MI (4 weeks post-treatment) (61.4 ± 3.0 vs. 47.6 ± 2.3 , $p=0.006$) (Supplementary Figure 1). LV end systolic volumes (LVESV) in the 2wk group also trended higher over this time period ($=61.7 \pm 32.4$ uL, $p=0.07$), suggesting ongoing remodeling and LV dilatation.

STG+EV Reduces Infarct Thinning and Preserves Ventricular Geometry

Frozen section analysis of hearts at 4 weeks post-MI with Masson's Trichrome demonstrated distinct transmural infarct in all hearts included in the analysis. All STG+EV treatment groups demonstrated attenuation of infarct thinning and had statistically significantly increased scar thickness compared to PBS alone. The 4 day group had the greatest scar thickness (0.885 ± 0.046 mm), which was statistically significantly increased compared to PBS (0.615 ± 0.029 mm, $p<0.0001$) and STG (0.577 ± 0.052 mm, $p<0.0001$) (Figure 6). Additionally, ventricular geometry was better preserved in the 3h (6.09 mm ± 0.44) and 4d

(6.20mm±0.73) groups, as indicated by smaller ventricular diameters compared to PBS (8.58mm±0.38, p=0.03, 0.04) or STG (9.13mm±0.25, p=0.01, 0.01).

DISCUSSION

Our group has previously demonstrated that STG+EV is a novel therapeutic with hemodynamic benefits when delivered to ischemic myocardium immediately following MI.⁶ We demonstrated that the EPC-derived EV reliably confers the same advantages of EPC therapy while overcoming many of the challenges to cell therapy and significant barriers to clinical translation. The use of STG further enhances the effect of the EPC-EVs by allowing precise targeting and sustained release of particles in addition to having intrinsic pro-angiogenic properties and providing mechanical stabilization of the peri-infarct region.

This study further informs and enhances the clinical applications of the STG+EV therapy by elucidating how timing of intervention affects resident cardiac cells' interaction with delivered EPC-EVs, and ultimately, the downstream functional and mechanical impact of therapy. By comparing outcomes after delivery of therapy at four timepoints after MI, we found the timing of delivery of STG+EV does indeed impact the degree of benefit derived.

In vitro studies showed improved responsiveness to STG+EV therapy in chronically hypoxic cells, suggesting that the compensatory mechanisms triggered by prolonged oxygen starvation, such as that experienced by cells in the borderzone of an infarct, primes cells to the pro-angiogenic factors within the STG+EV therapy. The increased responsiveness to EVs by preconditioned HUVECs may be due to and improved ability to uptake the delivered EVs. This suggests that the effective payload of 4d injections may be higher than that of 0hr injections due to more robust uptake by the resident cells in the ischemic myocardium.

Histologic analyses of hearts explanted at 4 weeks after MI demonstrated differences in scar thickness and ventricular geometry across treatment groups and controls, with less thinning of the infarct and mitigation of LV remodeling as indicated by preserved LV diameters in the 4d group. Hemodynamic assessment consistently demonstrated significant improvements in the group receiving therapy 4 days post-infarction. This timepoint correlates with the proliferative phase of the response to ischemic injury, and we hypothesized that the local environment within the myocardium at this point would be ideal for STG+EV delivery. H&E analysis of sections from 4 days post-MI demonstrates significant infiltration of inflammatory cells, which are crucial for clearance of dead cells from the infarct, and play an important role in tissue repair and regulation of the pro-inflammatory mediators.⁵ Given the predominance of inflammatory cells at 4 days post-MI and the strong effect of STG+EV therapy seen with intervention at this timepoint, it is possible that EPC-EVs play a role in immune modulation. Additional studies to further evaluate the interaction of EPC-EVs and immune cells after ischemic injury would be useful. Ultimately, the hemodynamic effects STG+EV on the primary outcome of Ees was greatest in the 4d group and was the only treatment group with statistically significant improvement over both PBS and STG controls. On additional measures of LV function, including dp/dt_{max} , dp/dt_{min} , EF, and cardiac output, treatment at 4 days appears to confer greater benefits than controls or other treatment timepoints. At the 4d timepoint, cells in the ischemic borderzone have likely initiated

compensatory measures and upregulated pro-survival pathways. Based on our *in vitro* data and pre-existing scientific knowledge regarding the progression of post-infarct inflammation and healing, delivery of STG+EV into this milieu should optimize the ability of cells to respond to the pro-angiogenic cargo of the EPC-EVs. STG delivery at this time also serves a critical role of stabilizing the weakened peri-infarct myocardium as cell death and necrosis progresses within the infarct.

The 2wk group initially demonstrated robust hemodynamics when assessed 4 weeks post-MI, however when re-assessed 2 weeks later, at 6 weeks post-MI (4 weeks post-treatment) there was deterioration of function. This is not surprising given histologic evidence that there is significant cell necrosis and evidence of the initial stages of fibrosis already present 2 weeks after MI. We hypothesize that STG delivered at this timepoint has significant bulking and mechanical unloading properties that may be especially important at this point in infarct evolution, when mechanical stress can further injure and deform vulnerable regions and lead to fibrosis. It is probable that the results at the early sac-point reflect effects of retained STG components, whereas the hemodynamics seen 4 weeks after treatment are a more accurate reflection of the ultimate effect of STG+EV treatment.

CONCLUSION

Overall, this study provides evidence that delayed intervention after MI with intramyocardial injection of STG+EV therapy into the infarct borderzone confers hemodynamic and structural benefits with delivery 4 days post-MI. We have shown evidence of a pro-angiogenic effect of EPC-EVs that is more pronounced with chronically rather than acutely ischemic cells. This may be due in part to the increased affinity for cell uptake of EPC-EVs after a prolonged period of hypoxia. The mechanical off-loading effects of STG likely also play a key role in preservation of scar thickness and ventricular systolic and diastolic function. Further studies to elucidate the mechanisms contributing to the differential effects of treatment at variable timepoints will help to guide engineering of the STG with regards to stiffness and degradation profile, as well as pinpointing the optimum time for delivery of EPC-EVs for maximum beneficial effect. As the possible therapeutic applications of EVs continues to expand, it is necessary to rigorously assess the optimal intervention strategy. This study helps to pinpoint the time at which post-MI intervention with STG+EV therapy can produce the most significant beneficial effect for preservation of ventricular contractility and structural integrity. The finding of optimal effectiveness occurring 4 days after MI improves the feasibility of clinical translation compared to immediate intervention.

LIMITATIONS

There are a few important limitations to note. Due to the numerous time points being evaluated, an STG-only control at each timepoint was not feasible and would have required a prohibitively large number of animals. Furthermore, there are benefits and shortcomings to defining a study endpoint based on time from MI as opposed to time from therapy. We chose a 4 week post-treatment, rather than post-MI, endpoint for all groups, to have a consistent time period over which the effects of the STG+EV therapy could be realized.

Supplementary Material

Refer to Web version on PubMed Central for supplementary material.

Acknowledgements

Funding provided by NIH NHLBI R01 (HL135090 – PI: Dr. Pavan Atluri), the Institute for Translational Medicine and Therapeutics, University of Pennsylvania (PI: Drs. Jason A Burdick and Pavan Atluri), F30 HL1344255 (Leo L. Wang). Anjali Patel contributed to data acquisition, analysis.

Biography



ABBREVIATIONS

Ad-HA	adamantane-modified hyaluronic acid
CD-HA	β -cyclodextrin-modified hyaluronic acid
Dp/dt	change in pressure over time
EES	end systolic elastance
EPC	endothelial progenitor cell
EPC-EV	endothelial progenitor cell-derived extracellular vesicle
ESPVR	end systolic pressure volume relationship
EV	extracellular vesicle
HA	hyaluronic acid
HUVEC	human umbilical vein endothelial cell
LAD	left anterior descending artery
LV	left ventricle
MI	myocardial infarction
PBS	phosphate buffered saline

STG	shear thinning gel
STG+EV	shear thinning gel and endothelial progenitor cell-derived extracellular vesicle construct
TBA	tetrabutylammonium hydroxide

REFERENCES

1. Kholia S, Ranghino A, Garnieri P, et al. Extracellular vesicles as new players in angiogenesis. *Vascul Pharmacol.* 2016;86:64–70. doi:10.1016/j.vph.2016.03.005. [PubMed: 27013016]
2. Coumans FAW, Brisson AR, Buzas EI, et al. Review Extracellular Vesicles Methodological Guidelines to Study Extracellular Vesicles. *Circ Res.* 2017;120:1632–1649. doi:10.1161/CIRCRESAHA.117.309417. [PubMed: 28495994]
3. Lamichhane TN, Sokic S, Schardt JS, Raiker RS, Lin JW, Jay SM. Emerging Roles for Extracellular Vesicles in Tissue Engineering and Regenerative Medicine. 2015;21(1):45–54. doi:10.1089/ten.teb.2014.0300.
4. Akers JC, Gonda D, Kim R, Carter BS, Chen CC. Biogenesis of extracellular vesicles (EV): exosomes, microvesicles, retrovirus-like vesicles, and apoptotic bodies. 2013:1–11. doi:10.1007/s11060-013-1084-8.
5. Frangogiannis NG. The inflammatory response in myocardial injury, repair, and remodelling. *Nat Publ Gr.* 2014;11(5):255–265. doi:10.1038/nrcardio.2014.28.
6. Chen CW, Wang LL, Zaman S, et al. Sustained release of endothelial progenitor cell-derived extracellular vesicles from shear-thinning hydrogels improves angiogenesis and promotes function after myocardial infarction. 2018;(June):1029–1040. doi:10.1093/cvr/cvy067.
7. Atluri P, Miller JS, Emery RJ, et al. Tissue Engineered, Hydrogel-Based Endothelial Progenitor Cell Therapy Robustly Revascularizes Ischemic Myocardium and Preserves Ventricular Function. *J Thorac Cardiovasc Surg.* 2014;148(3):1090–1098. doi:10.1021/ja8019214.Optimization. [PubMed: 25129603]
8. Gaffey AC, Chen MH, Venkataraman CM, et al. Injectable shear-thinning hydrogels used to deliver endothelial progenitor cells, enhance cell engraftment, and improve ischemic myocardium. *J Thorac Cardiovasc Surg.* 2015;19104. doi:10.1016/j.jtcvs.2015.07.035.
9. Li RK, Mickle DAG, Weisel RD, Rao V, Jia ZQ. Optimal time for cardiomyocyte transplantation to maximize myocardial function after left ventricular injury. *Ann Thorac Surg.* 2001;72(6): 1957–1963. doi:10.1016/S0003-4975(01)03216-7. [PubMed: 11789777]
10. Decicco-Skinner KL, Henry GH, Cataisson C, et al. Endothelial Cell Tube Formation Assay for the In Vitro Study of Angiogenesis. 2014;10(September):1–8. doi: 10.3791/51312.
11. Michiels C, Arnould T, Remacle J. Endothelial cell responses to hypoxia : initiation of a cascade of cellular interactions. *Biochim Biophys Acta.* 2000;1497.
12. Heikal L, Ghezzi P, Mengozzi M, Ferns G. Low Oxygen Tension Primes Aortic Endothelial Cells to the Reparative Effect of Tissue-Protective Cytokines. 2015:709–716. doi:10.2119/molmed.2015.00162.
13. Tian T, Zhu Y, Hu F, Wang Y, Huang N, Xiao Z. Dynamics of Exosome Internalization and Trafficking. *J Cell Physiol.* 2012;228(November):1487–1495. doi:10.1002/jcp.24304.
14. Atluri P, Miller JS, Emery RJ, et al. Tissue-engineered, hydrogel-based endothelial progenitor cell therapy robustly revascularizes ischemic myocardium and preserves ventricular function. *J Thorac Cardiovasc Surg.* 2014;148(3):1090–1098. doi:10.1016/j.jtcvs.2014.06.038. [PubMed: 25129603]
15. Pacher P, Nagayama T, Mukhopadhyay P, B atkai S, Kass DA. Measurement of cardiac function using pressure-volume conductance catheter technique in mice and rats. *Nat Protoc.* 2008;3(9): 1422–1434. doi:10.1038/nprot.2008.138. [PubMed: 18772869]

Central Message

EPC derived-extracellular vesicles in a shear thinning gel dramatically improve post-MI hemodynamics when delivered 4 days vs immediately post-infarct.

Perspective Statement

Endothelial progenitor cell-derived extracellular vesicles have great potential for widespread therapeutic applications in cardiovascular recovery after ischemic injury, but the optimal timing of intervention to maximize benefits remains unknown. This study demonstrates superior functional and mechanical properties with delayed injection of STG+EV 4 days after acute myocardial infarction.

Legend for Central Picture

Improved contractility (Ees) with 4-day delayed intervention with STG+EV injections after MI.

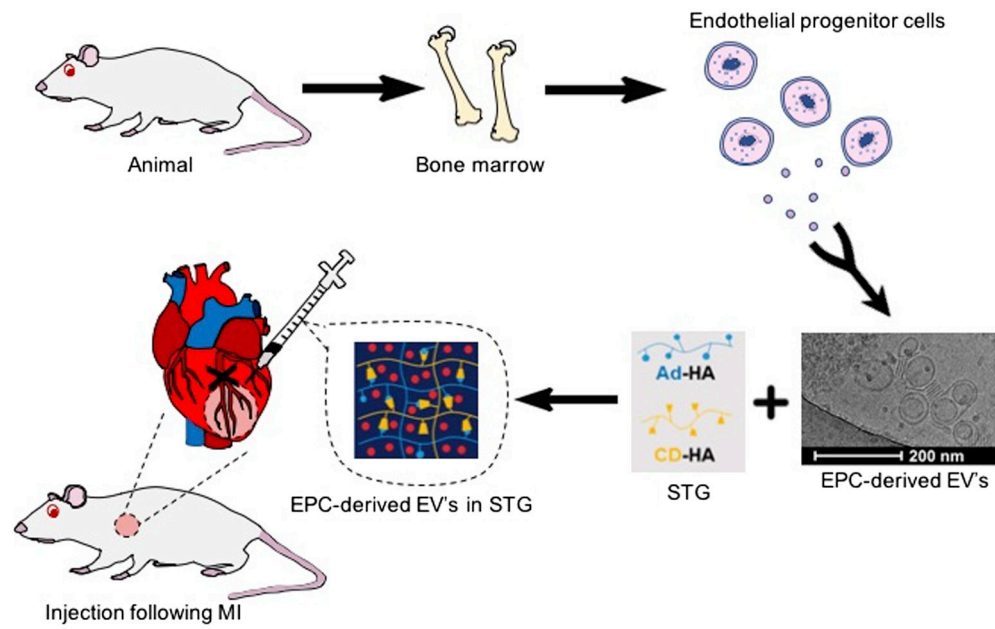


Figure 1. EPCs are harvested from the long bones of Wistar rats and plated.

EVs released from cells are isolated from CM. STG+EV is prepared by suspending EVs within STG. LAD ligation creates an LV infarct. At the designated post-MI intervention time, STG+EV is injected intramyocardially in the infarct borderzone. Post-treatment hemodynamics were assessed at 4 and 6 weeks post-MI.

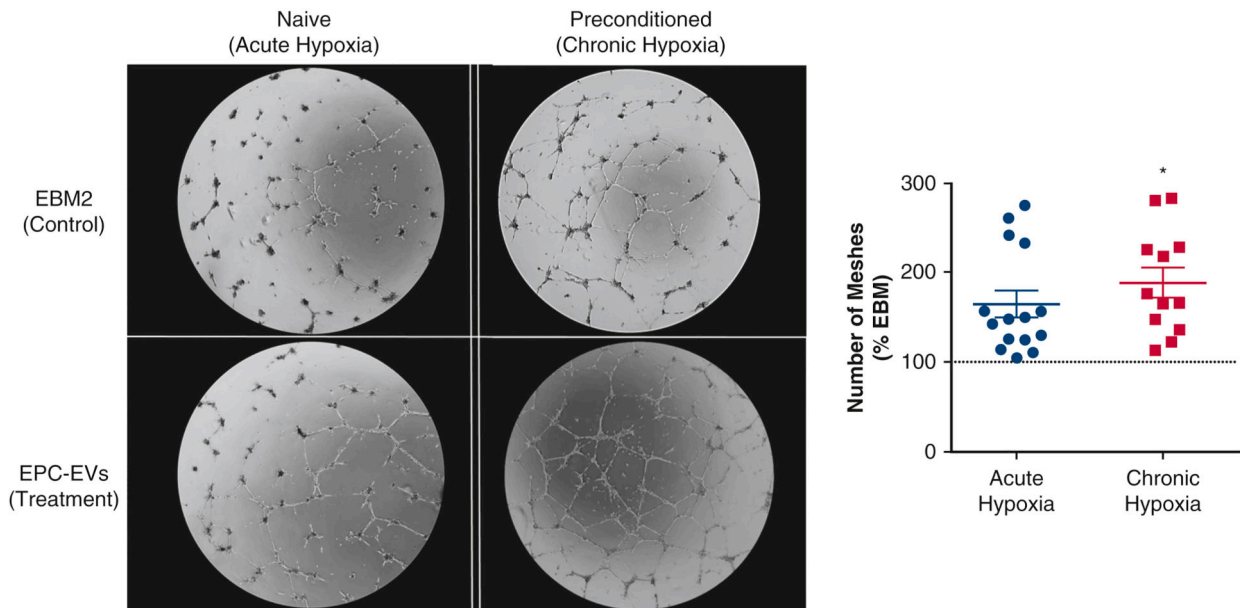


Figure 2. EPC-EVs promote a robust angiogenic response from chronically hypoxic HUVECs. HUVECS were exposed to chronic hypoxia (7 days, 5% O₂) to mimic an ischemic environment. Naive and preconditioned HUVECs were incubated with EVs in 5% O₂ for 14 hours. Chronically hypoxic HUVECs demonstrated increased vascular tubule mesh formation compared to the naive group (p=0.049).

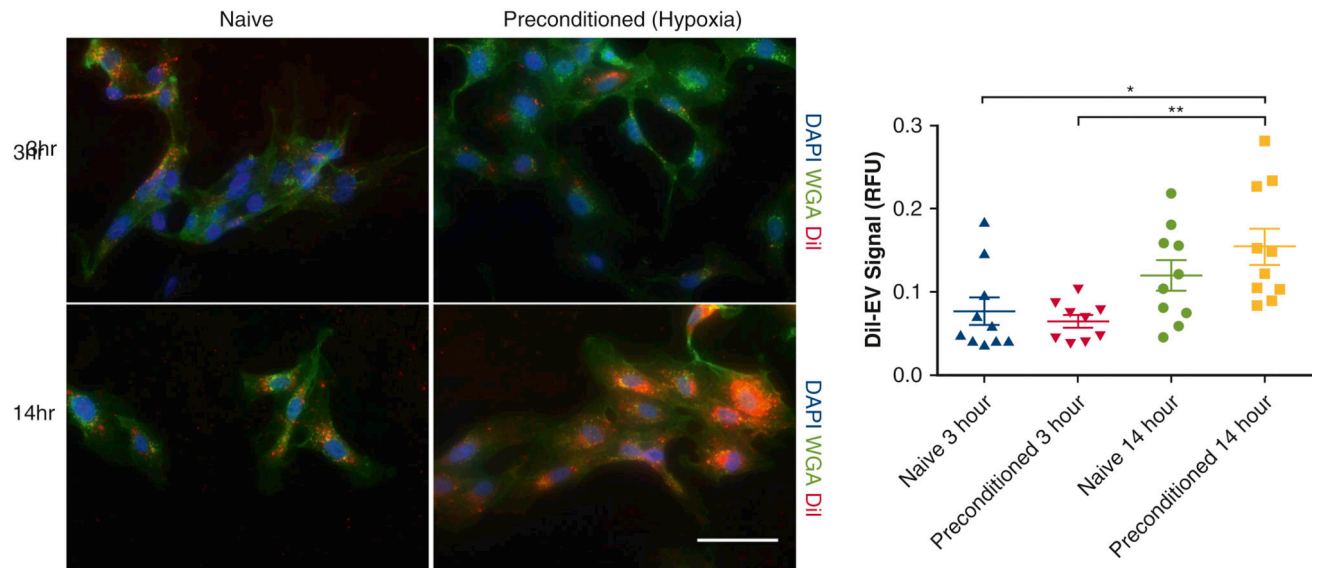


Figure 3. Hypoxic HUVECs demonstrate robust EPC-EV uptake ability. EPC-EV uptake by preconditioned HUVECS (4 days, 5% O₂) was compared to that of naive HUVECs at 3 and 14 hours after EPC-EV incubation in a hypoxic environment. After 14 hours, preconditioned HUVECs exhibited greater EV uptake than both naive ($p < 0.05$) and preconditioned ($p < 0.01$) cells in 3 hours of hypoxia.

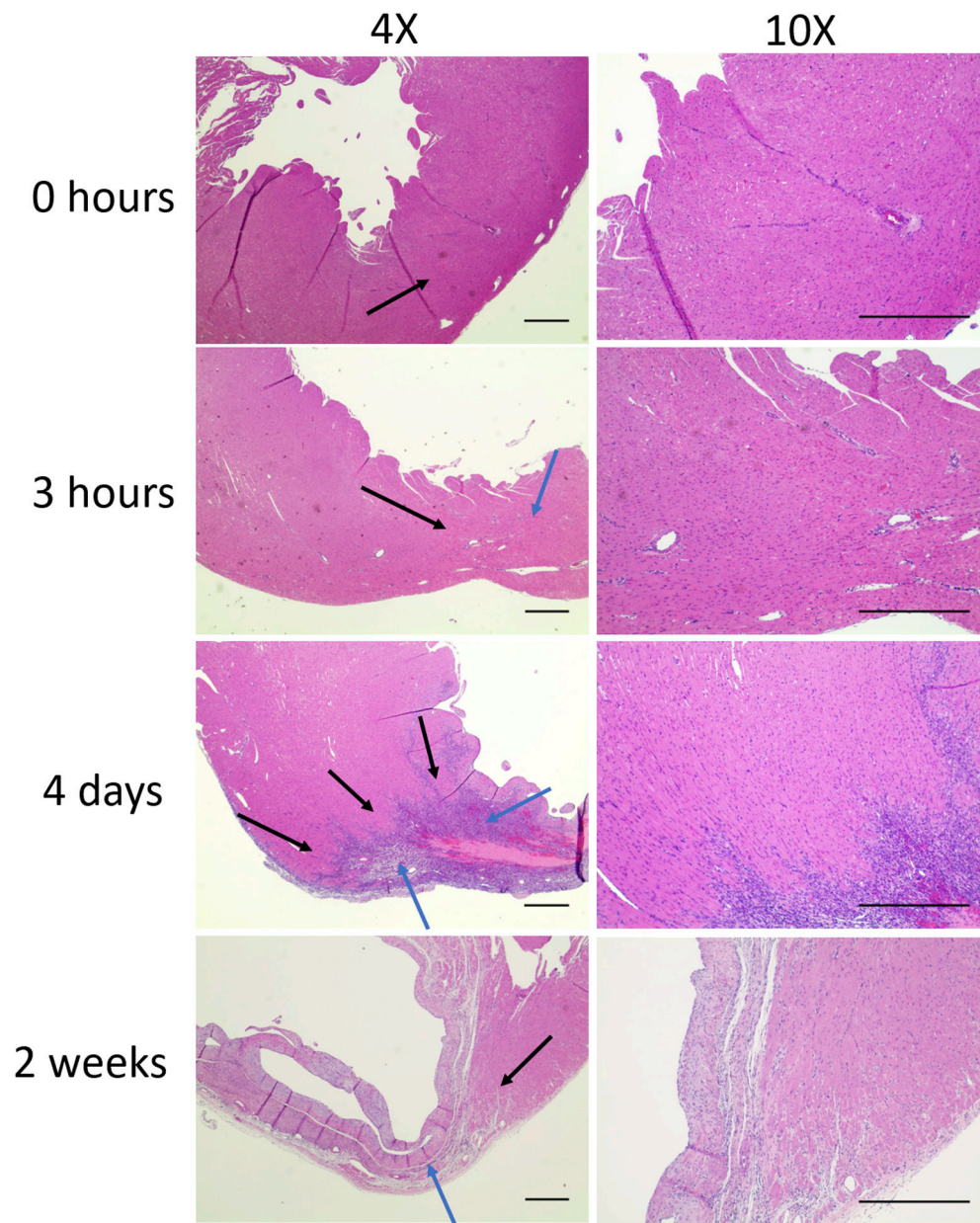


Figure 4. Representative H&E of infarct over time. Inflammatory cell infiltrate was evident at all timepoints. At 4 days there was delineation of scar and borderzone regions. Thinning of the LV wall from necrosis progressed in the 2 week group. Black arrows = borderzone. Blue arrows = infarct. Imaged at 4x and 10x magnification under brightfield. Scale 500um.

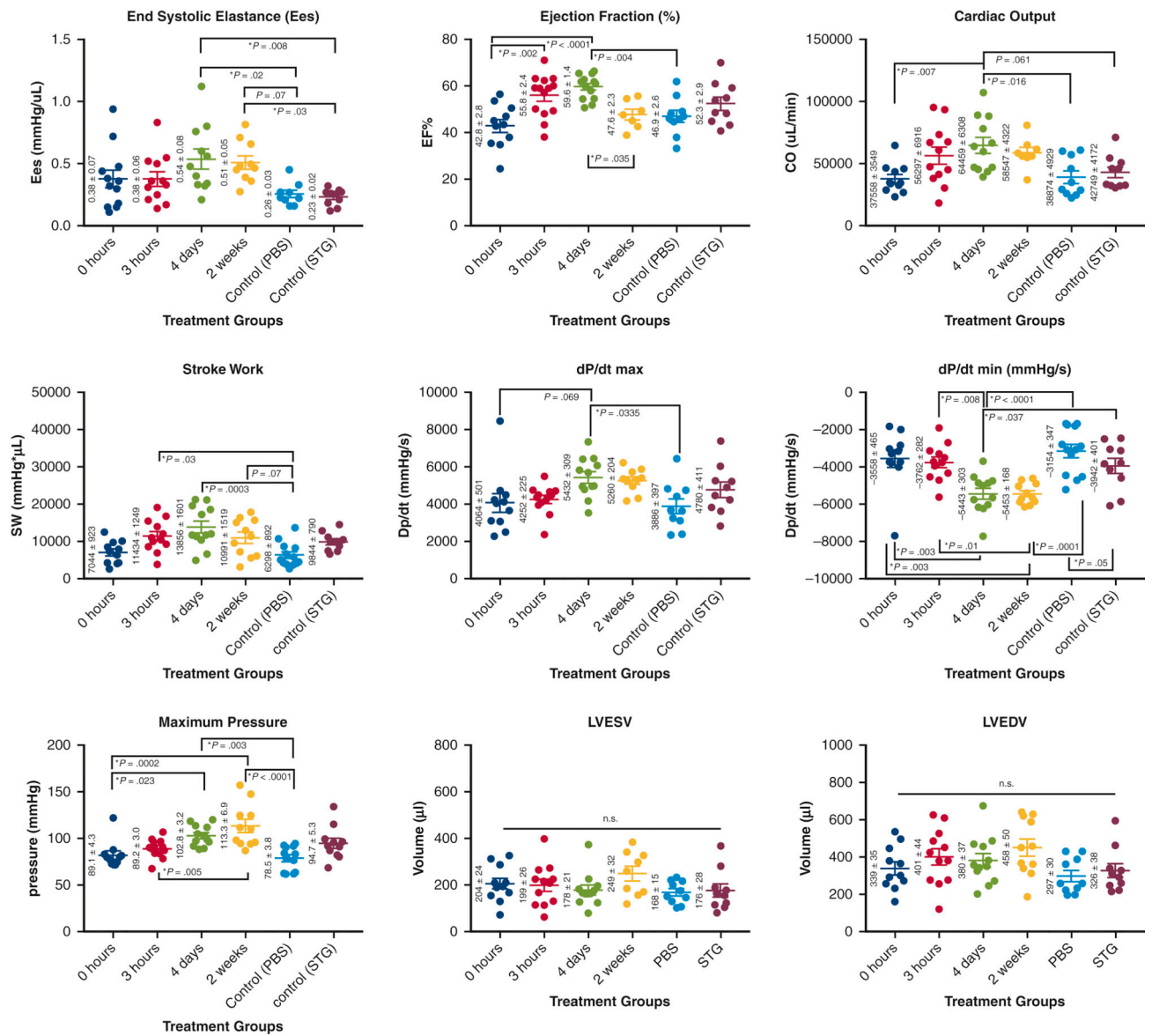


Figure 5. Hemodynamics panel. Data plotted as mean \pm SEM. Treatment groups indicate timepoints post-MI at which therapy was administered. Treatment at 4d post-MI shows greatest improvement in measures of Ees, EF, cardiac output, stroke work, and dP/dt max.

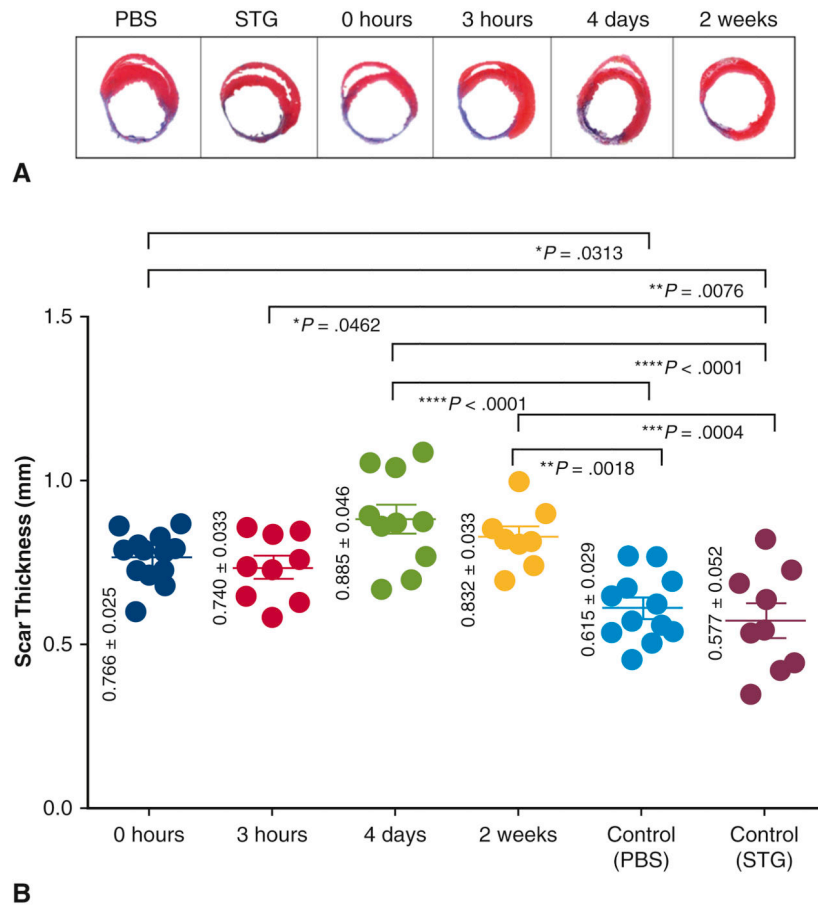


Figure 6. Delayed delivery of STG+EV limits infarct thinning.

A) Representative heart sections at 4 weeks post-MI were stained with Masson’s Trichrome.
 B) Scar thickness was calculated. The 4d group ($p < 0.0001$) had the greatest scar thickness compared to controls.

Table 1.

Summary table of hemodynamic data for each treatment group. Values are displayed as mean +/- SEM. Units shown in parentheses.

Treatment Group	Ees (mmHg/uL)	dP/dt max (mmHg/s)	EF (%)	CO (uL/min)	Stroke Work (mmHg*uL)	dP/dt min (mmHg/s)	Pmax (mmHg)	LVESV (uL)	LVEDV (uL)
pbs	0.26 +/- 0.03	3886 +/- 397	46.9 +/- 2.6	38874 +/- 4929	6298 +/- 892	-3154 +/- 347	78.5 +/- 3.8	167.6 +/- 15.3	297 +/- 29.9
stg	0.23 +/- 0.02	4780 +/- 411	52.3 +/- 2.9	42749 +/- 4172	9844 +/- 790	-3942 +/- 401	94.7 +/- 5.3	175.6 +/- 27.8	326.2 +/- 37.5
0 hour	0.38 +/- 0.07	4064 +/- 501	42.8 +/- 2.8	37558 +/- 3549	7044 +/- 923	-3558 +/- 465	89.1 +/- 4.3	204.9 +/- 23.5	339.1 +/- 35
3 hour	0.38 +/- 0.06	4252 +/- 225	55.8 +/- 2.4	56297 +/- 6916	11434 +/- 1249	-3762 +/- 282	89.2 +/- 3.0	199.2 +/- 26.1	400.7 +/- 43.6
4 day	0.54 +/- 0.08	5432 +/- 309	59.6 +/- 1.4	64459 +/- 6308	13856 +/- 1601	-5443 +/- 303	102.8 +/- 3.2	177.9 +/- 20.9	380 +/- 36.9
2 week	0.51 +/- 0.05	5260 +/- 204	47.6 +/- 2.3	58547 +/- 4322	10991 +/- 1519	-5453 +/- 168	113.3 +/- 6.9	248.5 +/- 31.6	458 +/- 50.2